RESEARCH ARTICLE

Adsorption of mercury from the aquatic environment using a novel nano-gel *of Descurainia Sophia* plant stem

Masoume Habibi[1], Arezou Ghadi[1,*], Soleiman Mahjoub[2]

[1]*Department of Chemical Engineering, Islamic Azad University, Ayatollah Amoli Branch, Amol, Iran.*

[2]*Clinical Biochemistry, Cellular and Molecular Biology Research Center, Health Research Institute, Babol University of Medical Sciences, Babol, Iran.*

ARTICLE INFO

Article History:
Received 2021-02-04
Accepted 2021-11-22
Published 2022-03-01

Keywords:
Mercury
Descurainia Sophia
Adsorption
Nano-gel
Thermodynamic
Isotherm

ABSTRACT

Mercury is one of the environmental toxic pollutants required to be removed. Mercury can interfere with the vital functions of the cells by binding to the sulfhydryl groups in enzymes and proteins. The purpose of this study was to investigate the adsorption of mercury ions from aqueous solutions using a novel adsorbent prepared by the nano-gel of *Descurainia Sophia* plant stem. Adsorption of mercury was performed in a discontinuous system. Detection of the adsorbent structure before and after the adsorption process was performed by SEM, TEM and FTIR analysis. The optimal mercury adsorption conditions were determined as 0.6 g/100 ml of mercury solution, the contact time of 100 min, and pH of 8. Under such conditions, the adsorption efficiency of 87.3% was obtained. Three parameters including Morris-Weber, pseudo-first-order, and pseudo-second-order kinetics were investigated to understand the kinetics of the removal process. Langmuir, Freundlich, and Dubinin-Radushkevich isotherms were also used to calculate adsorption capacity. The results showed that the nano-gel of *Descurainia* stem has a high ability to remove mercuric ions from aqueous solutions at different concentrations. Moreover, the temperature increase has a positive effect on the removal efficiency. The thermodynamic investigations indicate that the adsorption of mercury on the nano-gel of *Descurainia* stem was spontaneous and endothermic.

How to cite this article
Habibi M., Ghadi A., Mahjoub S. Adsorption of mercury from the aquatic environment using a novel nano-gel of Descurainia Sophia plant stem. J. Nanoanalysis., 2022; 9(1): 11-23. DOI: 10.22034/jna.2021.1922685.1248.

INTRODUCTION

Heavy metals in many parts of the world have been considered as environmental pollutants (in various physical and chemical forms and different concentrations) and have harmful effects on humans through the entry/evacuation of industrial wastewater and urban sewage into the environment. These materials such as cadmium, lead, and mercury are particularly dangerous because of their bioaccumulation in the body. These metals are concentrated in the food chain and cause an important risk for humans and animals [1, 2].

It is well-known that the toxicities of heavy metals are different in different conditions and depend on factors such as concentration, environmental conditions, contact time, and other physical, chemical, and biological factors. Heavy metals not only pollute the water consumed by humans and creatures, but also cause severe soil contamination. In some cases, due to the contamination of metallic material, the lands lose their value to agriculture. Moreover, the existence of these metals in the environment can lead to groundwater pollution due to dispersion in the soil. Most heavy metals in biological reactions interfere with the cells of living organisms. The presence of these metals in municipal sewage also disrupts wastewater treatment systems, reduces the efficiency of the treatment, and in some acute cases can stop the biological activities of the purification systems [1-3].

* Corresponding Author Email: *arezoo.ghadi@Gmail.com*

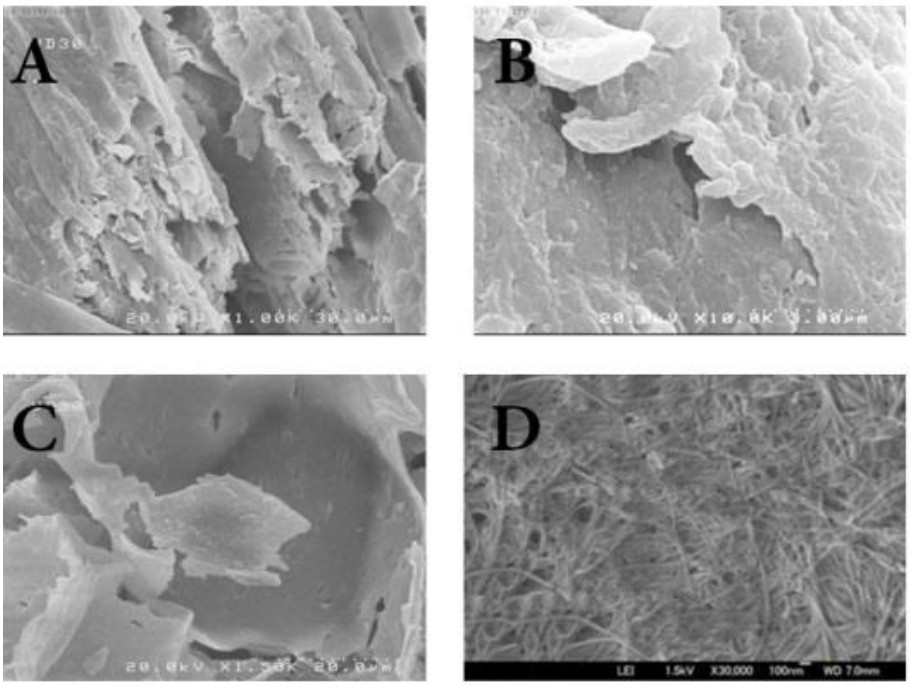

Fig. 1. SEM image of the adsorbent sample used with the magnification of 1000 times (A). An electron microscope image of the adsorbent sample was used with the magnification of 10,000 times (B). Absorbent electron microscope image, with the magnification of 1.5k (C). Transmission Electron Microscope (TEM) image of the nanostructure of nano-gel adsorbent (D).

One of these heavy metals is mercury that present in the metallic, mineral, and organometallic forms in the environment. Mineral mercury is in the form of one and two-grade salts. Double-capacity of this metal is more frequent than single-capacity, in the environment. Alkaline waters also provide suitable conditions for the production of dimethylmercury that is highly volatile and reactive. Dimethylmercury is one of the strongest known neurotoxins and is easily absorbed through the skin. Mercury is one of the toxic substances that interferes with the vital functions of the cells by binding to the sulfhydryl groups in enzymes and proteins. The metal mercury vapor is absorbed through the human skin at a rate of 0.024 ng Hg/cm^2 of skin per milligram of airborne mercury [3].

In the past few years, sustained development and attention to the next generation have led researchers to investigate methods that help reduce environmental degradation and the spread of pollution. However, the industries lead to more pollution release in the environment. Comprehensive reviews of previous actions suggest that inexpensive adsorbents, not only are available, but also possess high adsorption capacity [1]. There are many reports based on the study of the optimum adsorption conditions, the type of material as adsorbent, the conditions of suitable environments for adsorption, and the ability of the adsorbent to be converted to active carbon [2]. Natural adsorbents such as living organisms-derived adsorbents, e.g., Artemia or plants exist mainly in nature. Typically, these types of adsorbents are derived from the shell or their body components such as bone, hair, and skin. In this field, a well-known adsorbent is chitosan which known as a biopolymer, obtained from the hard skin of chitin-like artemia [1, 2]. Overall, natural adsorbents have attracted the attention of many experts, due to their abundance in nature and their excellent adsorption ability. Many agricultural products, and plant and animal wastes such as leaves and seeds, and the peel of fruits are abundantly produced in nature, and because of the ability to recover and return to the ecosystem cycle of these materials, using them as adsorbent has become much more profitable and comfortable. From the Chemistry viewpoint, such adsorbents are materials such as chitosan/chitin [4], carbon derived from the indium sedimentation [5] bran ash activated by bentonite [6], vertebrate species [7], the raw wood of the pine tree, and improved wood with acid [8].

The purpose of this study was to use a nano-gel of *Descurainia* plant stem, as an effective and

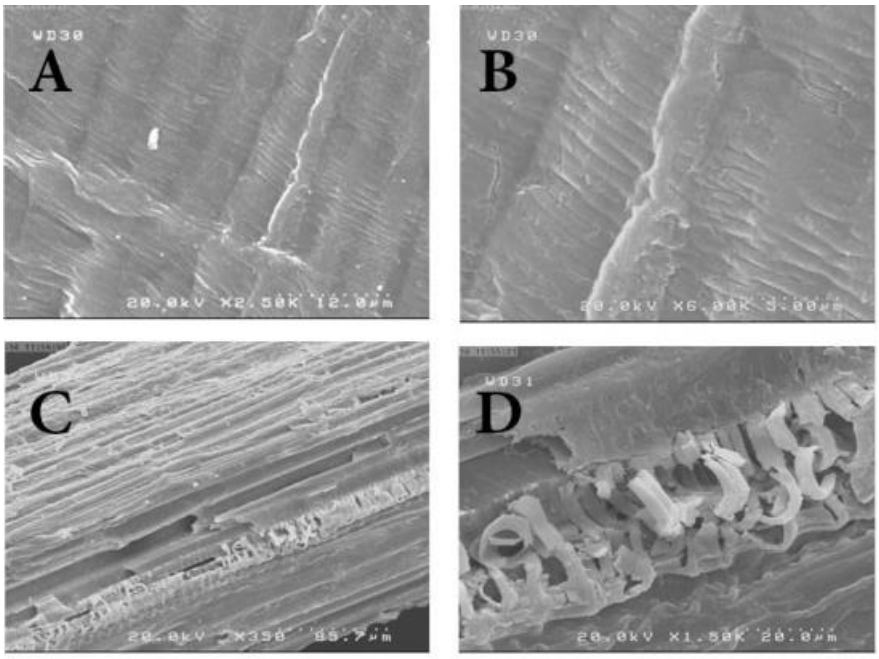

Fig. 2. Cellulosic fibers are arranged in regular intervals with a magnification of 2.5 K (A) and in a regular manner, like woven fabric, with a magnification of 6K (B). SEM image of the adsorbent before gelting, after being added to the chlorine admixture of 1 mol and with a residual time of 1 h with a magnetic stirrer at 150 rpm, with a magnification of 350 times (C). SEM image of the adsorbent before gelting, after being attached to the 1 molar additive with 1 mol of chloride and 1 hour with a magnetic stirrer at 150 rpm, with a magnification of 1.5K (D).

inexpensive adsorbent for the removal of mercury from aqueous solutions. The effect of efficient parameters in the adsorption process such as pH, contact time, adsorbent mass, and initial concentration of mercury in this study was also investigated.

MATERIALS AND METHODS

Materials

All materials and solvents such as Mercury(II) chloride (HgCl2), Hydrochloric acid (HCl), Sodium hydroxide (NaOH were purchased from Merck Chemical Company.

Methods

Preparation of Descurainia Sophia nano adsorbent

The initial adsorbent material used in this study was *Descurainia Sophia*, which was approved by the Herbarium of Agricultural University after its approval. *Descurainia Sophia*, common names include flixweed, herb-Sophia, and tansy mustard, is a one-year-old or two-year-old plant and a member of the mustard family. *Descurainia Sophia* grows in the plains and mountains, and the height of the stem reaches up to one meter. The bottom of the plant is fluffy, while its top is not. The seed of this plant is tiny and slightly long and usually has two colors; one of them is red, which has a little bitter taste, and the other is dark red.

To prepare the nano-gel, the top-down method was used. For the preparation of nano-gel adsorbent, two milling and crushing steps were necessary. To prepare the adsorbent, first, the obtained stems were washed to remove any dust and contaminants and then completely dried. The dried stems were crushed to smaller sizes by an electric mill, then the adsorbent grading was carried out using the standard sieve sample 60.

To treat the adsorption, the adsorbent was placed in a mesh size range of 60 mg chloride 1 mol for 1 hour, on a stirrer at 150 rpm to activate the active adsorption sites. In the next step, 100 g of this adsorbent was used for transferring into a super mill. The second stage included the use of the Japanese Super Disk Milling, which was considered as a sensitive phase, due to the high pressure that converted the size of the mesh to nano dimensions. For the disc mill, the feeding to the mill was slowly carried out, and most parts of the input feeding were performed using DM (double distillation) water to prevent solids and dirt contained in the adsorbent that was left in the absorbent cavity after

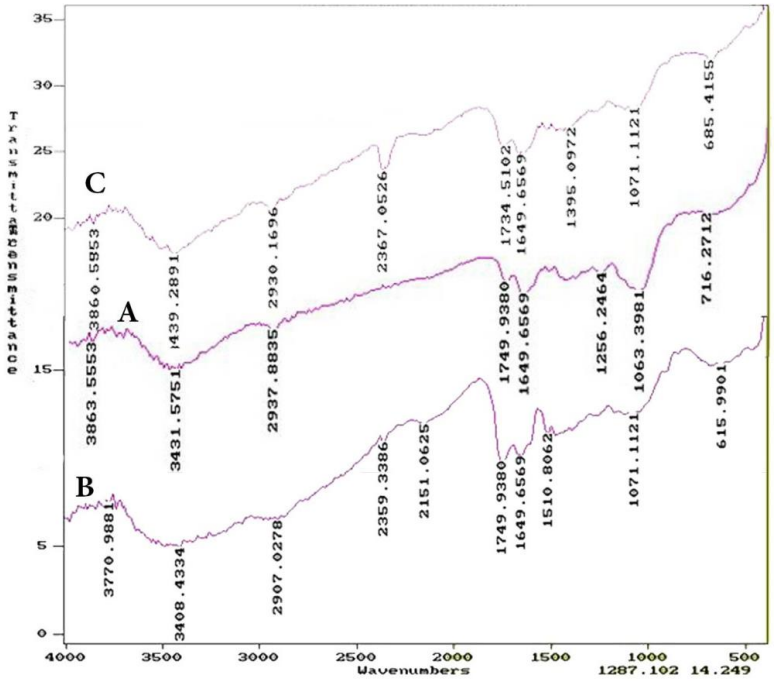

Fig. 3. (A) The FTIR spectrum of the second form of adsorbent without adding acid. (B) Adsorbent FTIR spectrum after immersion in hydrochloric acid 1 M. (C) The adsorbent FTIR spectrum upgraded after mercury adsorption from aqueous solution.

the washing.

The distance between the two discs in this device is very close, and the two disks are in the opposite direction and it is roughly at 1500 rpm. Hence, any irregularity at rotation time and very hard objects can damage the discs. All of the grinded material in the first stage should be at a point that passed through the mesh 60. Considering the loss in the second stage of the mill, due to the lack of feed, about 400 g of nano-gels were produced. This value was enough to complete all the experiments. Followed by, nano-gels were used to perform mercury adsorption experiments. It is notable that due to the presence of water content for this type of adsorbent, the percentage of water was determined by water percentage experiments. In brief, a certain amount of the nano-gel was weighted and then placed inside the oven at the temperature of 70 °C for 12 h. The amount of water used in the nano-gel was 90%, which was exactly the same as the percentage of water added in the Nano Novin Polymer Company.

Adsorbent Characterization

Scanning Electron Microscope (SEM) device was used to identify the adsorbent surface and morphology. Before the SEM assessment, the surface of the adsorbent was coated with a thin layer of gold to improve SEM images and achieve higher-quality images.

The identification of functional groups was also carried out by Fourier transform infrared (FTIR). To this end, 1 mg of adsorbent was uniformly mixed with 1000 mg of KBr, then pressed on a plate under the pressure of 200 kg/cm^2 for 5 min. Finally, the sample was analyzed. The scan range of specimens was between 500-4000 cm^{-1}.

Adsorption experiments

To prepare a solution of mercury in different concentrations, a solution of $HgCl_2$ (1000 mg/L) was prepared, and then, diluted to various concentrations. The HCl and NaOH were used to adjust the pH of the solution.

Adsorption experiments were carried out discontinuously using a mixer. The volume of all solutions used was 100 ml and after each experiment, the solvent and adsorbent filtration was removed and the sample was prepared for analysis. Each experiment was repeated twice and its results were compared to each other (the error rate for each test: below 5%). Mercury concentration was measured using atomic absorption spectroscopy (Model, country).

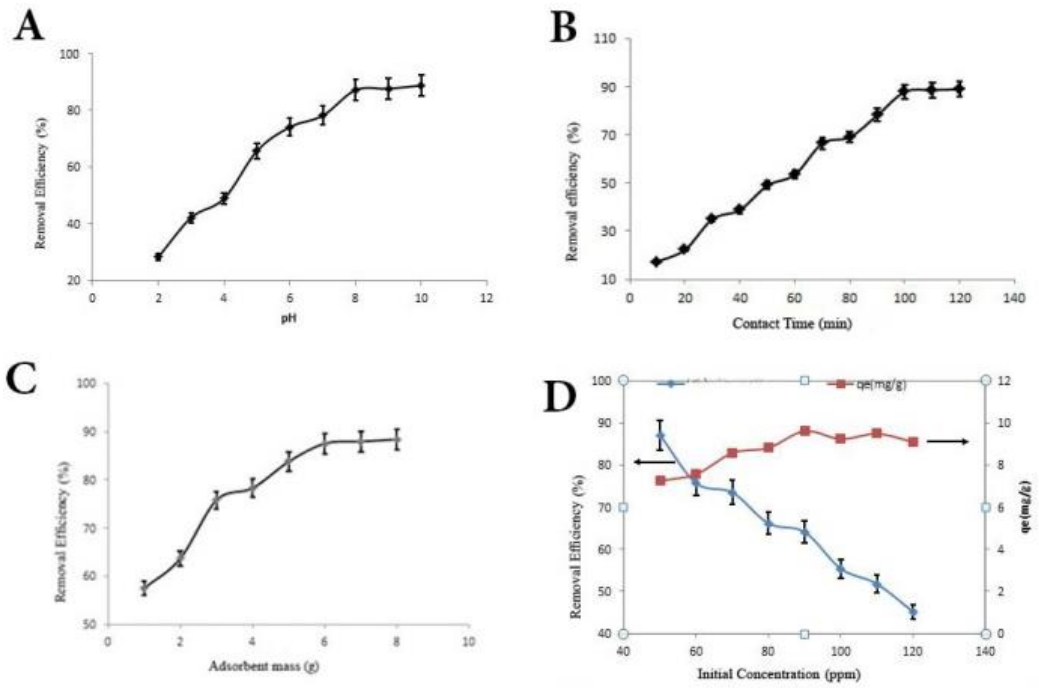

Fig. 4. (A) The effect of pH on the efficiency of removal of mercury by the adsorbent. (B) The effect of contact time on the removal efficiency of mercury by the adsorbent. (C) The effect of adsorbent in an aqueous solution on the efficiency of removal of mercury by the adsorbent. (D) The effect of initial concentration on the adsorption capacity of mercury by the adsorbent.

The adsorption efficiency for the series of experiments is obtained from the equation (1).

$$\%\,Removal = \frac{(C_i - C_f)}{C_i} \times 10 \qquad \text{Eq. (1)}$$

In which Ci is the initial concentration and Cf is the final concentration of the adsorbed material. To calculate the amount of adsorbed mercury at time t, we can use equation (2):

$$q_t = (C_i - C_t) \times \frac{V}{m} \qquad \text{Eq. (2)}$$

In this equation, qt (mg/g) is the amount of mercury adsorbed per unit mass of the adsorbent at time t, Ct (mg/L) is the concentration of mercury in solution at time t, V (L) is the volume of solution and m (g) is the mass of the adsorbent.

The calculation of the amount of mercury ion adsorbed by the adsorbent during equilibrium can use a similar relationship from equation (2)

$$q_e = (C_i - C_e) \times \frac{V}{m} \qquad \text{Eq. (3)}$$

In equation (3), qe (mg/g), is the amount of mercury adsorbed per unit mass of the adsorbent during equilibrium, and Ce (mg/L) is the concentration of mercury in the solution at equilibrium time.

Measuring of the mercury ions concentration using atomic adsorption

The atomic adsorption method is done in two methods: flame and graphite furnace. The atomic adsorption method is one of the most important techniques that can be used for the analysis of about 70 metal elements with excellent accuracy and sensitivity.

RESULTS AND DISCUSSION

Investigating the adsorbent structure

Morphology of the SEM device

An electron microscope was used to investigate the shape and size, as well as the uniformity of surface and appearance of the adsorbent and the adsorbent particles (Fig. 1). However, for the nano-gels, an electron microscope was used due to a lack of solidification. Fig. 1 A-D and fig. 2 A-D represent the adsorbent with mesh 60 (before the conversion to the nano-gel), with different magnifications. As it is shown in the figures, the porosity is high in the adsorbent and the size of the cavity reaches a few microns. In addition, the plant's stem has a

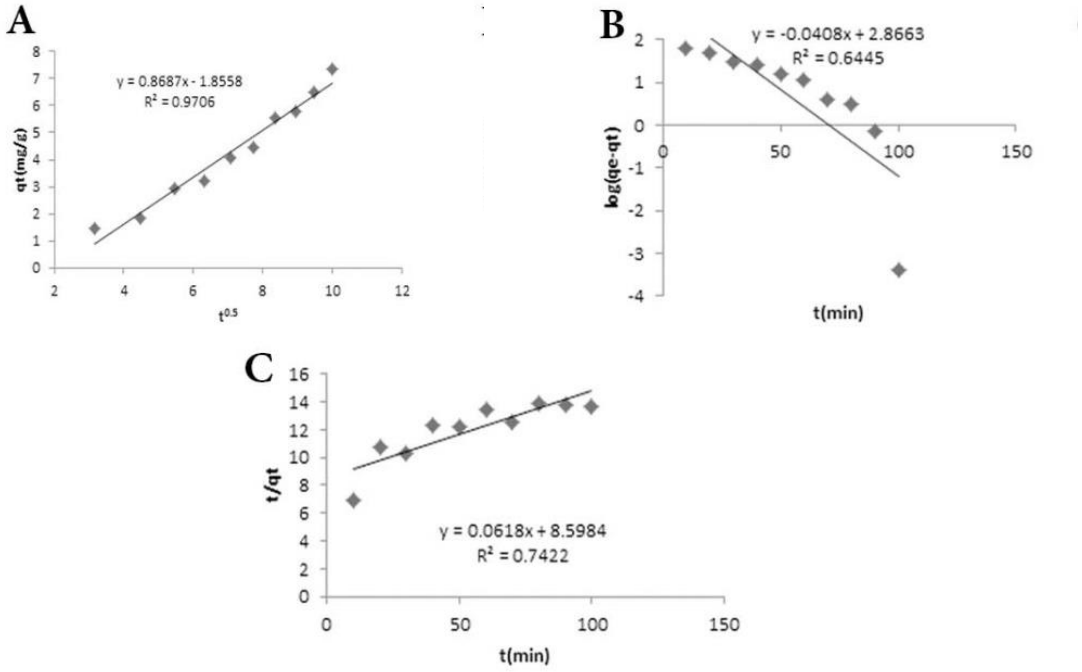

Fig. 5. (A) Characterization of a Morris-Weber linearized equation for adsorbing mercury on the adsorbent. (B) Drawing a pseudo-first-order linearized equation for adsorbing mercury on the adsorbent. (C) Drawing of the pseudo-second-order linearized equation for absorbing mercury on the adsorbent.

lot of cavities, the walls of the cavities are also very porous, which is well illustrated in Fig. 1C.

The role of lignin is the framework for the main body that prevents the bending and softening of the plant during growth and afterward, and causes the plant to always be standing tall and raised. Lignin, as the hardest element in the plant, prevents the reaching adsorbate to the adsorbed areas [9]. In the present study, after converting the adsorbent in the form of a nano-gel, one of the preventing barriers of the adsorbate adsorption was removed.

To prepare adsorbent with a nano-structure, some of it became in the form of a nano-gel. In this form, the particles were completely uniform and the particle size was much smaller and the cavities disappeared (Fig. 2). It can be seen in Fig. 2, such that the fibers and cellulosic fibers have tangled and woven into the *Descurainia Sophia* structure. It is the same lignin that hardens the adsorbate adsorption into the internal holes. Fig. 2 also shows the cellulosic fibers with a magnification of 6000 times, that are arranged regularly, like woven fabric. After adsorbing (the acid before the gelation process), some of the adsorbent lignin was lost and this factor was also affected by better adsorption. Accordingly, the adsorbent with a nano-structure leads to a better interaction between adsorbate and adsorbent.

FTIR analysis

The FTIR spectrometer provides important information about the types and the foundations of the biocompatible polymer structure and the types of composites. Therefore, the FTIR spectrum of the adsorbent was studied. The results have shown in Fig. 3 A-C.

Examples of adsorbents performed by FTIR analysis include:

Sample 1: *Descurainia sophia* without acid treatment (before the gelation process and meshed with sieve 60 mesh)

Sample 2: *Descurainia sophia* with acid treatment (before the gelation process and meshed with sieve 60 mesh and pickled)

Sample 3: Adsorbent after adsorption of mercury from aqueous solution

A negative charge was induced on the adsorbent by adsorbent acidification, which caused metal cation to be well adsorbed by the adsorbent and increased the adsorption rate.

For Sample 1 (Fig. 3 A), the peak of 716 cm^{-1} represents the C-H group attached to the benzene ring. The 1063.3 cm^{-1} peak is related to the bending vibration of the carbon-carbon double bond in

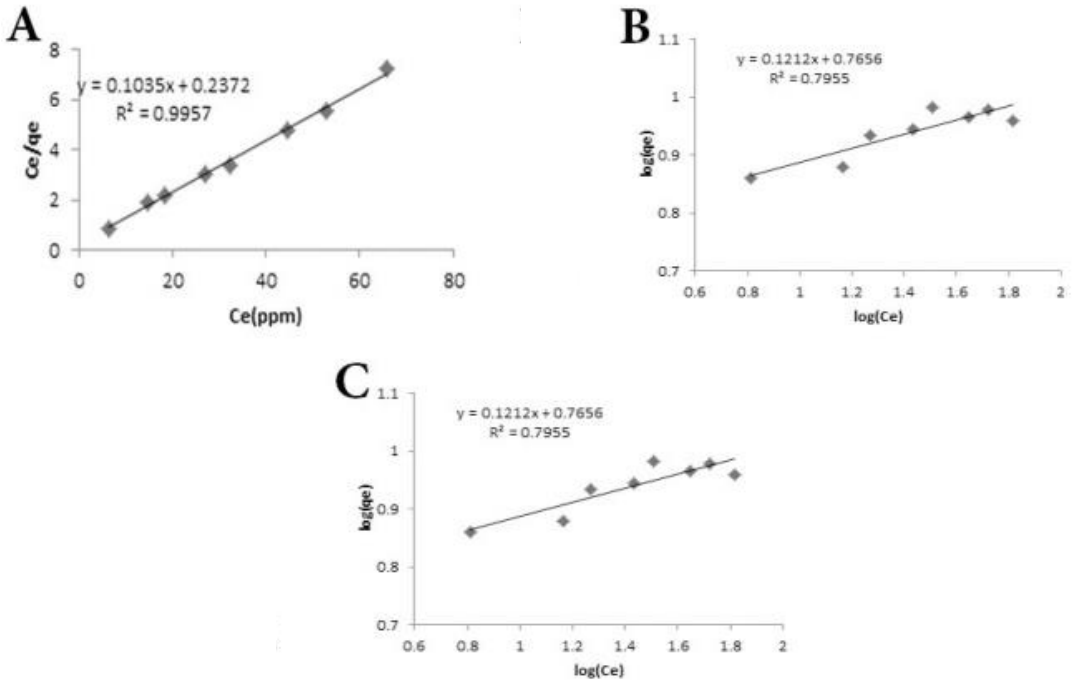

Fig. 6. (A) The construction of a Langmuir linearized equation for adsorbing mercury. (B) The drawing of the Freundlich linearized equation for mercury on the adsorbent. (C) Drawing of a D-R linearized equation for adsorbing mercury on the adsorbent.

the aromatic ring (C=C), which is more precisely related to 2-methoxy-2-phenyl ethanol. The peak at 1256 cm^{-1} is related to the internal CH or silica compounds, and 1649.6 cm^{-1} is related to the water-adsorbed group. Likewise, 1749.9 cm^{-1} refers to the carbon-oxygen bond in the carbonyl group (C=O) [10]. It should be noted that in the range of 3300 to 3400 cm^{-1}, this group also generates a peak (not so recognizable). The peak of 2937.8 cm^{-1} is also related to carbon group 4 that linked to the chlorine or bromine halogens. The peaks of 3431.5 cm^{-1} and 3863.5 cm^{-1} are assigned to the O-H bond of adsorbed water on the adsorbent and external C-H bond, respectively.

In Fig. 3 B, 616 cm^{-1} peak is related to the presence of magnesium and aluminum hydroxide, which is probably due to the presence of magnesium hydroxide and aluminum in the chloride-containing acid. 1071 cm^{-1} is associated with the CO-linkage in the polysaccharide structure. The peaks of 1510 cm^{-1} and 1649 cm^{-1} are also related to the C-C bond in the aromatic ring, and the adsorbed water group, respectively. The peaks of 1749 cm^{-1} and 2151 cm^{-1} are related to the carbon-oxygen bond in the carbonyl group that adsorbed on the hydroxyl [11]. The 2907 cm^{-1} peak is related to the C-H bond of dimethylsilyl group, and 3408.4 cm^{-1} peak is assigned to the chloride bond in $CHCl_3$, which was created due to adsorption of glucose in chloride [9]. The peak at 3770 cm^{-1} is also related to the hydroxyl bond in the AlOH structure and or oxygen-hydrogen bond is related to humidity.

In Fig. 3 C, the peaks at 685.4cm^{-1}, 1071cm^{-1}, and 1395 cm^{-1} are related to the external C-H gradient, the C-O bond in the polysaccharide structure, the O-H bond, respectively. The peak at 1649 cm^{-1} is related to the adsorbed water group. Moreover, the 1734cm^{-1} peak is related to the carbon-oxygen bond in the carbonyl group [12]. The peaks at 2367 cm^{-1}, 2930cm^{-1}, and 3439 cm^{-1} are related to the C≡N bond, the external C-H bond, and the O-H bond, respectively. Likewise, 3770 cm^{-1} is related to hydroxyl in the structure of AlOH or oxygen-hydrogen bonding is related to humidity. According to Fig. 4 B and C, it can be concluded that the adsorbent structure in the adsorption process has not changed much. Therefore, the adsorption of mercury by this adsorbent can be considered as physical adsorption.

Effect of pH on Removal Efficiency

The pH of the solution is one of the most important adsorption factors. The pH is usually effective in three ways: adsorbent surface load,

Table 1. isotherm equation and constants of adsorption isotherms for adsorbing mercury on the adsorbent.

Langmuir Equation	K_L (min^{-1})	q_O (mg/g)	R^2
	0.4363	9.66	0.9957
Freundlich Equation	K_F (min^{-1})	N	R^2
	5.83	8.25	0.7955
Dubinin Radushkevich Equation	B	q_m	R^2
	0.000002	9.09	0.6617

ionization degree, and change in the nature of the adsorbent during the process.

The effect of pH on the adsorption of mercury from an aqueous solution was investigated by the nano-stem of *Descurainia Sophia* plant (at the pH range of 2-10) (Fig. 4 A). Experiments were carried out at an initial concentration of 50 ppm, a contact time of 240 min, and at 20 °C. The amount of adsorbent in 100 ml of the mercuric aqueous solution was 10 g. As shown in Fig. 4 A, the adsorption process of mercury by adsorbent strongly depends on the pH. Such that, with increasing pH from 2 to 8, the removal efficiency increased to its maximum and at pH ≥ 9, a significant change was not observed in the mercury removal efficiency. The replacement of hydrogen ions on the adsorbent surface with mercury cationic molecules in an aqueous solution is accorded due to an increase in the amount of mercury adsorption at high pH levels. The concentration of hydrogen ions is one of the most important parameters in the absorption process. At low pH values, the reduction in adsorption rate was observed due to the higher mobility of hydrogen ions than metal ions.

The high mobility of hydrogen ions leads to a reaction of these ions with the active adsorption solutions, prior to metal ions [13]. At low pHs, the negative sites of the adsorbent also decrease, and consequently the number of positive sites of the adsorbent surface increases. As a result, the ions Hg^{+2} and $Hg(OH)^{+}$ are not adsorbed by the adsorbent [13].

Effect of the reaction time on the removal efficiency

The effect of the reaction time on the adsorption of mercury using the *Descurainia Sophia* plant stem nano-gel is shown in Fig. 4 A. The test conditions were pH of 8, initial concentration of 50 ppm, adsorbent 10 g per 100 ml. As shown in this Figure, the adsorption efficiency increases with increasing the duration of the contact time until the achievement of the equilibrium, and it did not change significantly. In justifying this phenomenon, it can be said that at the beginning of the reaction, with increasing contact time, the adsorbent possesses more chance of penetrating the adsorbent and occupying active adsorption sites. When the process is balanced, the adsorbent is being saturated, and increasing the contact time does not affect the adsorption efficiency. Regarding the Figure, the equilibrium time for this process is 100 min, the adsorption efficiency at this time is equal to 87.9%. Based on the results, the reaction time in the next experiments for adsorption of mercury by the adsorbent was selected 100 min.

Investigation of Adsorption Kinetics

Many adsorption phenomena are dependent on time. To understand the dynamics of the reaction and predict the rate of adsorption with time, evaluation of the kinetics of these processes are very important. Several kinetic models are used for adsorption in discontinuous processes, but due to the mathematical complexity of these models, they can not be easily applied. In this regard, reactions that change qt based on time, are easier for the kinetics of adsorption. Models used in this field are Morris-Weber pseudo-kinetic model, first-order, and pseudo-second-order models. Notably, in the quasi-first-order equation, it is assumed that the difference between qt and qe is the main propulsion force for the adsorption action, and the adsorption rate is proportional to this force.

Morris-Weber Kinetic Model

Morris-Weber equation is also used to

Table 2. Effect of temperature on the removal efficiency of mercury by the adsorbent.

(°C) Temperature	Removal Efficiency (%)
20	87.3
30	89.8
40	90.7
50	92.4

investigate the influence of penetration in the kinetics of the process. The process of adsorption of particles from aqueous solution onto the adsorbent occurs in several steps, and the final adsorption process may be controlled by one or more steps. The first step involves the penetration of the adsorbent from the solution to the external surface of the adsorbent. The penetration of the cavity is the second stage, and if this is known as the controlling step, this phenomenon can be studied using the Morris-Weber equation. The third stage is penetrated at the adsorbent surface. In this stage, the final equilibrium is based on the very low concentration of adsorbent in solution and the loss of active sites in the adsorbent.

Morris-Weber equation was presented as follows (4) [14]:

$$q_t = K_{id}(t)^{0.5} + C \qquad \text{Eq. (4)}$$

q_t (mg/g) is the adsorption rate at time t(min), $K_{id}(mg/(g.min)^{1/2}$ is the constant of internal penetration, and C is the constant of the boundary layer thickness. The qt vs. $t^{0.5}$ is shown in Fig. 5 A.

The k_{id} can be obtained by calculating the slope of the line. The Morris-Weber equation for adsorbing mercury on the nano-gel of *Descurainia Sophia* plant stem was K = 0.8687 min^{-1} with the correlation coefficient of 0.9706.

Pseudo-First-Order Kinetic Model

The pseudo-first-order equation is as shown in equation (5) [15]:

$$\frac{dq_t}{dt} = k_1(q_{eq} - q_t) \qquad \text{Eq. (5)}$$

$q_t\left(\frac{mg}{g}\right)$ and $k_1\frac{1}{min}$ are the absorption rate at time t and constant of the first-order equation, respectively. The linear form of equation 5 was provided in equation 6.

$$log\ log\ (q_e - q_t) = logq_e - \frac{k_1 t}{2.303} \qquad \text{Eq. (6)}$$

In the pseudo-first-order equation, the intensity of the filling of adsorbent sites is proportional to the number of vacant sites and propulsion power and is considered linear.

The K_1 is obtained with the drawing of $\log(q_e\text{-}q_t)$ vs. t. (Fig. 5 B). Based on the results, the constant of pseudo-first-order equation for adsorbing mercury on the nano-gel of *Descurainia Sophia* plant stem and correlation coefficient were K_1=0.094 min^{-1}, 0.6445, respectively.

Pseudo-Second-Order Kinetic Model

Pseudo-second-order equation is based on the amount of equilibrium capacity, in which the intensity of filling of the adsorbent sites is assumed to be proportional to the square of the number of vacant adsorbent sites (Eq. 7) [16]. The linear form of this equation was provided in equation 8

$$\frac{dq_t}{dt} = K_2(q_{eq} - q_t)^2 \qquad \text{Eq. (7)}$$

$$\frac{t}{q_t} = \frac{1}{k_2 q_e^2} + \frac{t}{q_e} \qquad \text{Eq. (8)}$$

$K_2(gmg^{-1}min^{-1})$ is constant of pseudo-second-order equation. The parameters K_2 and q_e are obtained by drawing the $\frac{t}{q_t}$ vs. t.

The constant of the pseudo-second-order equation and the correlation coefficient were obtained 0.00044 min^{-1} and 0.7422, respectively (Fig. 5 C). Comparing the data showed that the results are well correlated with the Morris-Weber equation and the adsorption process is controlled

Table 3. Thermodynamic parameters of mercury adsorption on the adsorbent.

	ΔH (kj/mol)	ΔS (kj/molK)	T °C	ΔG (kj/mol)	R^2
			20	-4.696	
Hg(II)	15.08	0.067	30	-5/4797	0.9782
			40	-5.9268	
			50	-6.7081	

by this equation.

It is notable that the degree of removal metal directly depends on the presence of adsorbent in aqueous solution and its concentration in aqueous solutions. Moreover, in penetration mode, in the second stage, penetration is based on the high concentrations of adsorbents in a large amount. As previously mentioned, the results are very consistent with the Morris-Weber kinetic equation. This also indicates that the stage of limiting of adsorption rate in this reaction is the intramolecular penetration stage.

Effect of Adsorbent mass on The Removal Efficiency

To determine the amount effect of adsorbent on the removal efficiency of mercury by the nano-stem of the *Descurainia Sophia* plant, different amounts of nano-gel in 100 ml of the aqueous solution containing a concentration of 50 ppm of mercury and optimum pH and contact time were assessed. As can be seen in Fig. 4 C, with increasing the amount of adsorbent from 1 g to 6 g, the removal efficiency has increased and the increase of more than 6 g led to a little effect on the removal efficiency. Therefore the amount of 6 g of the adsorbent in 100 ml of the aqueous solution is selected as the optimum adsorbent mass. It is notable that the increased adsorption efficiency by increasing the amount of adsorbent can be explained by the increase in the number of active sites available on the adsorption and consequently the adsorption efficiency increases. However, after passing the optimal time, the solution reaches equilibrium and the increase in adsorbent mass will not affect the adsorption efficiency.

Effect of initial concentration on the adsorption process

To investigate the effect of initial concentration on the adsorption process, different concentrations of mercury aqueous solutions were prepared and the adsorption process was carried out under optimal conditions. The initial concentration range was chosen between 120-150 ppm. As observed in Fig. 4 D, the increased mercury concentration in the solution, led to an increase in the adsorption capacity. Although, after the concentration of 100 ppm, the adsorption capacity remained almost constant, and little changes were observed. Indeed, when the concentration increases, the lack of active sites and surface leads to less adsorption. Moreover, it can be said, the number of these sites is constant, when the ion concentration increases, adsorption sites are filled and the adsorption capacity increases, but in more concentrations, and when all sites are filled, the increase in concentration will not affect the adsorption capacity [17].

Adsorption Isotherms

In the adsorption isotherm is assumed that all adsorption sites are the same and independent of other sites, whether these sites be empty or filled with the adsorbate. Isotherms show the relationship between the adsorbate concentration in the solution and its amount on the adsorbent, at a constant temperature. The Langmuir, Freundlich, and Dubinin-Radushkevich isotherms were used to study the constancy of isotherms.

Langmuir Isotherm

The Langmuir theory describes the monolayer coating of the adsorbate on the homogeneous adsorbent surface. This isotherm is based on the assumption that the adsorption action for each site occurs only once. Langmuir equation is in the form of the following equation [18].

$$q_e = \frac{q_0 K_L C_e}{(1+K_L C_e)} \qquad \text{Eq. (9)}$$

Where qe, Ce, and q_o are the equilibrium

Table 4. Comparison of the maximum mercury adsorption capacity (qm) on the stem nano-gel of Descurainia Sophia plant with other adsorbents.

No.	Adsorbent Name	Maximum adsorption Capacity (mg/g)	Ref.
1	Stem Nanogel of *Descurainia Sophia* Plant	9.66	In This Study
2	Carbon Sulfur	4.5	[19]
3	Almond peel	0.0058	[20]
4	Powder palm shell	62.9	[21]
5	Ceramic	0.00065	[22]
6	Bonded Polyethylene thiol	7.02	[23]

adsorption capacity, the equilibrium concentration, and the maximum amount of single-layer adsorption (the qo can also be called theoretical adsorption capacity), respectively. The linear form of this isotherm to obtain the Kc and q_o, indicated in Equation (10).

$$\frac{C_e}{q_e} = \frac{1}{q_0 .K_L} + \frac{1}{q_0} C_e \qquad \text{Eq. (10)}$$

The q_o and K_L obtain by drawing C_e/q_e vs. Ce (Fig. 6 A). As it can be seen in this Figure, the gradient of the line is positive, and the correlation coefficient is very high (Table 1). It indicates that this equation is very suitable for this adsorption process.

Freundlich Isotherm

The Freundlich isotherm is based on a non-homogeneous or heterogeneous surface. In this isotherm, it is assumed that the enthalpy has a logarithmic decrease with the increase in the number of sites occupied. Non-linear and linear equations of Freundlich isotherm indicate equations 11 and 12 [18].

$$q_e = K_F\ (C_e)^{1/n} \qquad \text{Eq. (11)}$$

$$log(q_e) = log(K_F) + \frac{1}{n}\ log(C_e) \qquad \text{Eq. (12)}$$

K_F and 1/n are the Freundlich constant and adsorption intensity, respectively.

The n and K_F were obtained from the log(qe) vs. log (Ce) curve. Fig. 6 B shows the linear model of this equation for mercury adsorption on the nano-gel of the *Descurainia Sophia* stem. The results are presented in Table 1. In this equation, when n is between 1 and 10, the adsorption process indicates an optimal process.

The Dubinin Radushkevich model

The Dubinin Radushkevich model was used for data analysis. The linear form of this model was presented in Equations 13 and 14 [13].

$$ln\ ln\ (q_e)\ = ln\ ln\ (q_m)\ - \beta\varepsilon^2 \qquad \text{Eq. (13)}$$

$$\varepsilon = RT\ ln\ [1 + \left(\frac{1}{C_e}\right)] \qquad \text{Eq. (14)}$$

In this equation, q_e, q_m, β, and ε are is the equilibrium adsorption capacity, the maximum of the adsorption capacity of the theory, the constant of the equation, and the Polanyi potential.

By drawing the linear form of ln(qe) vs. ε^2, β and q_0 were obtained (Fig. 6 C). The results of this experiment are listed in Table (1).

The average value of energy is obtained using the equation E= $\frac{1}{\sqrt{2\beta}}$, in which this value to adsorb mercury on the adsorbent was 0.5 $kJmol^{-1}$. Since the value of E is smaller than 8 $kJmol^{-1}$, it can be said that physical adsorption has occurred. By examining these three isotherms, it was found that experimental data are in good agreement with the Langmuir model. This suggests that Langmuir's hypothesis for mercury adsorption by nano-gel of *Descurainia Sophia* stem is dominant, and the adsorption process of the mercury was performed as a monolayer.

Effect of Temperature

The effect of temperature on adsorption efficiency was investigated at the temperature range of 20-50 °C. To perform mercury adsorption using nano-gel of *Descurainia Sophia* stem, the following settings were applied.

The contact time of 100 min, the adsorbent mass of 6 g in 100 ml, the initial mercury concentration of 50 ppm. The results are listed in Table 2. It was found, with increasing temperature, the removal efficiency increases, although, this amount was minor.

Indeed, the temperature increase, promots the absorption rate of the adsorbate onto the adsorbent, because with increasing temperature, the thickness of the boundary layer (around the adsorbent) is increased, hence, the transfer of the adsorbate from the solution on the adsorbent active sites is easily accomplished, which results in the increased adsorption efficiency. The positive effect of the temperature on the removal efficiency indicates that the mercury adsorption reaction is thermosensitive.

Thermodynamics of the process

The thermodynamics of absorption processes were studied using the data in Table 2. The parameters of Gibbs free energy (ΔG) and entropy (ΔH) and entropy (ΔS) were calculated by the equations (15), (16), and (17).

$$K_c = \frac{F_e}{1-F_e} \qquad \text{Eq. (15)}$$

$$log\ log\ K_c = \frac{-\Delta H}{2.303RT} + \frac{\Delta S}{2.303R} \qquad \text{Eq. (16)}$$

$$\Delta G = -RT\ ln\ ln\ K_c \qquad \text{Eq. (17)}$$

In equation (15), Fe is a part of a water-soluble substance that is absorbed by the adsorbent. The thermodynamical parameters of the mercury adsorption process by the nano-gel of the *Descurainia Sophia* stem are presented in Table 3. As can be seen, ΔG is negative, the negative value of this parameter shows that the removal of mercury by the studied adsorbent is a spontaneous adsorption process. A positive value of ΔH also indicates that the process is thermosensitive. Likewise, the positive value of ΔS demonstrates increased randomness at the solid-liquid phase, during the adsorption of the ions on the adsorbent surface.

Adsorbent Comparison with Other Adsorbents

The comparison of maximum adsorption capacity of nano-gel of the *Descurainia Sophia* stem with other studies was carried out and the results are listed in Table 4.

It was found that the *Descurainia Sophia* stem nano-gel-derived adsorbent in removing mercury provides a higher adsorption rate than adsorbers of sulfur-treated carbon, almond peel, ceramic, and Polyethylene thiol. Therefore, it can be said, the adsorbent prepared in this study due to its low economic value is very suitable for the removal of mercury from aqueous solutions.

CONCLUSION

In conclusion, improving the adsorbent was performed by two physical and chemical methods, the first adsorbent was produced using a top-down method of the primary material with a mesh 60 in the form of a nano-gel. The adsorbent was chemically treated before conversion into a nano-gel and then was acidified with acid chloride. For nano-gel adsorbents, due to the adsorption of nano-sized particles, the mass transfer resistance was lost. The identification of the structure of *Descurainia Sophia* plant stem was performed before and after the adsorption process, by FTIR. The results indicated that the adsorbent structure was unchanged after the adsorption process, which indicates the physical nature of the adsorbent is stable. The pH of 8 was obtained as optimal pH, for this adoption process. The exposure time for the adsorption of mercury on the adsorbent was 100 min. The kinetic results of the adsorption process showed better compliance with the Mauritius-Weber model. The balance data also showed good compliance with Langmuir isotherm. Investigating the effect of initial concentration on the adsorption capacity showed that the adsorption process of mercury possesses the maximum adsorption capacity at 100 ppm concentration. Followed by that, investigation of the temperature effect on the adsorption process and its thermodynamic showed that the adsorption process is spontaneous and endothermic

DECLARATION OF COMPETING INTEREST

The authors declare that there are no conflicts of interest.

FORMATTING OF FUNDING SOURCES

This research did not receive any specific grant

from funding agencies in the public, commercial, or not-for-profit sectors.

REFERENCES

1 Sabino De G, Giusy L, Mariangela G, Michele N. Characteristics and adsorption capacities of low-cost sorbents for wastewater treatment: A review. Sustainable Materials and Technologies. 2016; 9: 10-40 https://doi.org/10.1016/j.susmat.2016.06.002

2 Gupta V. Application of low-cost adsorbents for dye removal-A review. Journal of environmental management. 2009; 90: 2313-2342. https://doi.org/10.1016/j.jenvman.2008.11.017

3 Charles T.D, Robert P.M, Hing Man C, Daniel J.J, Nicola P. Mercury as a Global Pollutant: Sources, Pathways, and Effects. Environ. Sci. Technol. 2013; 47: 4967–4983. https://doi.org/10.1021/es305071v

4 Guijuan J, Weiwei B, Guimei G, Baichao A, Haifeng Z, Shucai G. Removal of Cu (II) from aqueous solution using a novel crosslinked Alumina-Chitosan hybrid adsorbent. Chinese Journal of Chemical Engineering. 2012; 20: 641-648. https://doi.org/10.1016/S1004-9541(11)60229-2

5 Sivasankar V, Rajkumar S, Murugesh S, Darchen A. Tamarind (Tamarindus indica) fruit shell carbon: A calcium-rich promising adsorbent for fluoride removal from groundwater. Journal of hazardous materials. 2012; 225: 164-172. https://doi.org/10.1016/j.jhazmat.2012.05.015

6 Visa M. Tailoring fly ash activated with bentonite as adsorbent for complex wastewater treatment. Applied Surface Science. 2012; 263: 753-762. https://doi.org/10.1016/j.apsusc.2012.09.156

7 Sánchez-Martín J, Beltrán-Heredia J, Gragera-Carvajal J. Caesalpinia spinosa and Castanea sativa tannins: A new source of biopolymers with adsorbent capacity. Preliminary assessment on cationic dye removal. Industrial Crops and Products. 2011; 34: 1238-1240. https://doi.org/10.1016/j.indcrop.2011.03.024

8 Dawood S, Sen T K. Removal of anionic dye Congo red from aqueous solution by raw pine and acid-treated pine cone powder as adsorbent: equilibrium, thermodynamic, kinetics, mechanism and process design. Water research. 2012; 46: 1933-1946. https://doi.org/10.1016/j.watres.2012.01.009

9 Paul Langan(Principal Investigator) A A, G. Bellesia, and A. Bradbury. Making Fuels from Plants, Los Alamos, USA, p. 2 (2012).

10 Schrenk W. Analytical atomic spectroscopy, Springer Science & Business Media 2012.

11 Reynolds R J, Aldous K, Thompson K. Atomic absorption spectroscopy: a practical guide, Griffin London1970.

12 Okuno D, Iwase T, Shinzawa-Itoh K, Yoshikawa S, Kitagawa T. FTIR detection of protonation/deprotonation of key carboxyl side chains caused by redox change of the Cu(A)-heme a moiety and ligand dissociation from the heme a3-Cu(B) center of bovine heart cytochrome c oxidase. Journal of the American Chemical Society. 2003; 125: 7209-7218. https://doi.org/10.1021/ja021302z

13 Ghodbane I, Hamdaoui O. Removal of mercury (II) from aqueous media using eucalyptus bark: Kinetic and equilibrium studies. Journal of Hazardous Materials, 2008; 160: 301-309. https://doi.org/10.1016/j.jhazmat.2008.02.116

14 Weber WJ, Morris JC. Kinetics of adsorption on carbon from solution. Journal of the Sanitary Engineering Division. 1963; 89: 31-60. https://doi.org/10.1061/JSEDAI.0000430

15 Lagergren S. Zur theorie der sogenannten adsorption geloster stoffe. Kungliga svenska vetenskapsakademiens. Handlingar. 1898; 24: 1-39.

16 Bhattacharya A, Naiya T, Mandal S, Das S. Adsorption, kinetics and equilibrium studies on removal of Cr (VI) from aqueous solutions using different low-cost adsorbents. Chemical engineering journal. 2008; 137: 529-541. https://doi.org/10.1016/j.cej.2007.05.021

17 Katal R, Hasani E, Farnam M, Baei MS, Ghayyem MA. Charcoal ash as an adsorbent for Ni (II) adsorption and its application for wastewater treatment. Journal of Chemical & Engineering Data. 2012; 57: 374-383. https://doi.org/10.1021/je200953h

18 Reynolds T D. Unit operations and processes in environmental engineering, Brooks 1977.

19 Hsi H-C, Rood M J, Rostam-Abadi M, Chen S, Chang R. Effects of sulfur impregnation temperature on the properties and mercury adsorption capacities of activated carbon fibers (ACFs). Environmental science & technology. 2001; 35: 2785-2791. https://doi.org/10.1021/es001794k

20 Khaloo S S, Vosoughi S, Gholamnia R. Efficiency comparison of two types of almond shell in removal of mercury from aqueous solution. Journal of Kermanshah University of Medical Sciences (J Kermanshah Univ Med Sci). 2013; 17: 155-163.

21 Kushwaha S, Sodaye S, Padmaja P. Equilibrium, kinetics and thermodynamic studies for adsorption of Hg (II) on palm shell powder. Proceedings of World Academy of Science, Engineering and Technology. 2008; p: 617-623.

22 Bhakta J, Salim M, Yamasaki K, Munekage Y. Mercury adsorption stoichiometry of ceramic and activated carbon from aqueous phase under different pH and temperature. ARPN J Eng Appl Sci. 2009; 4: 52-59.

23 Saad D M, Cukrowska E M, Tutu H. Selective removal of mercury from aqueous solutions using thiolated cross-linked polyethyleneimine. Applied Water Science. 2013; 3: 527-534. https://doi.org/10.1007/s13201-013-0100-7